tvst

https://doi.org/10.1167/tvst.8.3.51

Article

Quantitative Discrimination of Healthy and Diseased Corneas With Second Harmonic Generation Microscopy

Francisco J. Ávila[1], Pablo Artal[1], and Juan M. Bueno[1]

[1] Laboratorio de Óptica, Instituto Universitario de Investigación en Óptica y Nanofísica, Universidad de Murcia, Murcia, Spain

Correspondence: Juan M. Bueno, Universidad de Murcia, Laboratorio de Óptica, Campus de Espinardo (Ed. 34), Murcia 30100, Spain. e-mail: bueno@um.es

Received: 17 September 2018
Accepted: 30 April 2019
Published: 27 June 2019

Keywords: nonlinear microscopy; stroma organization; corneal pathologies

Citation: Ávila FJ, Artal P, Bueno JM. Quantitative discrimination of healthy and diseased corneas with second harmonic generation microscopy. Trans Vis Sci Tech. 2019; 8(3):51, https://doi.org/10.1167/tvst.8.3.51

Purpose: To analyze the spatial organization of pathological corneas with second harmonic generation (SHG) imaging and to provide a proof of concept to objectively distinguish these from the healthy corneas.

Methods: A custom-built SHG microscope was used to image the anterior stroma of ex vivo corneas, both control and affected by some representative pathologies. The structure tensor (ST) was employed as a metric to explore and quantify the alterations in the spatial distribution of the collagen lamellae.

Results: The collagen arrangement differed between healthy and pathological samples. The former showed a regular distribution and a low structural dispersion (SD $< 40°$) within the stroma with a well-defined dominant orientation. This regular arrangement drastically turns into a disorganized pattern in pathological corneas (SD $> 40°$).

Conclusions: The combination of SHG imaging and the ST allows obtaining quantitative information to differentiate the stromal collagen organization in healthy and diseased corneas. This approach represents a feasible and powerful technique with potential applications in clinical corneal diagnoses.

Translational Relevance: The ST applied to SHG microscopy images of the corneal stroma provides an experimental objective score to differentiate control from pathological or damaged corneas. Future implementations of this technique in clinical environments might might be a promising tool in Ophthalmology, not only to diagnose and monitor corneal diseases, but also to follow-up surgical outcome.

Introduction

The cornea is the main ocular refractive element, composed of five histologically differentiated layers. The stroma makes up approximately 90% of the corneal thickness[1] and it mainly consists of type I collagen fibers, arranged in a particular organization to maintain the shape, transparency, and biomechanical properties of the cornea.[1–3]

Second harmonic generation (SHG) microscopy is a noninvasive imaging technique suitable for visualizing label-free collagen-based tissues, in particular the human corneal stroma.[4–6] This imaging technique has been established as an efficient tool to accurately investigate the three-dimensional collagen structure of the cornea at high spatial resolution.[7,8] Moreover, SHG provides a detailed visualization of the stroma structures not seen under commercially available devices based on linear confocal microscopy.[9]

The distribution of the corneal collagen is modified under different circumstances, such as pathologies, surgery, scarring, and wound healing. Alterations of this intrinsic organization might seriously compromise the regular optical and metabolic functions. SHG microscopy has been reported to detect collagen structural abnormalities in corneas suffering from pathologies, such as keratoconus,[10–14] keratitis,[15–17] edema,[18] bullous keratopathy,[19,20] or fibrosis.[21,22]

The effects of some corneal diseases are not readily visible, and the patients are only aware of it at late stages, when the visual function is significantly reduced. In that sense, an objective index to distinguish between healthy and pathological corneas is highly recommended for clinical applications.

Different methods have been used to analyze the

collagen structural organization (see Ref. 23 as general review). A few of them have been used to quantitatively explore the changes in corneal morphology under different experimental conditions. In particular, the fast Fourier transform (FFT) is the most popular tool to quantify corneal collagen distribution from SHG images. This approach has been used to analyze changes after external thermal damage[24] or corneal cross-linking,[25,26] to study differences between healthy and keratoconic corneas[11,13] as well as to evaluate the condition of human corneas before transplantation.[27] To explore healthy donor corneal tissue Lombardo et al.[28,29] used a tensorial mathematic approach providing numeric parameters (inhomogeneity index, scalar order) and an anisotropy index measurement. Other algorithms to evaluate collagen patterns are also available, these include the Radon transform,[30] the degree of waviness,[31] and texture analyses.[32]

Here, we propose the use of the structure tensor (ST)[33] as an objective and quantitative method to differentiate healthy from pathological corneas. This is based on the analysis of SHG images of ex vivo corneas under a variety of experimental conditions. Healthy specimens used as control are compared with corneas with different diseases to demonstrate its validity.

Materials and Methods

SHG Microscope

A detailed description of the custom SHG microscope used for the purpose of this work can be found elsewhere.[34] In brief, a mode-locked laser system (wavelength 760 nm) was combined with a scanning unit and an inverted microscope to acquire SHG images of ex vivo corneas. The SHG signal was recorded in the backward direction via the same microscope objective (×20, Numerical Aperture [NA] = 0.5) and reached the detection unit after passing a narrow-band spectral filter. A step Z-motor, coupled to the objective allowed moving the focus along the sample's depth if required, with an axial resolution of 1 μm/step. The SHG images shown in this work correspond to a total area of 210 × 210 μm^2 for a size of 256 × 256 pixels. Every final SHG image was the result of the average of three individual frames to reduce noise effects.

Samples

The samples involved in this study corresponded to 12 ex vivo corneas. The control healthy human corneas used were not suitable for transplantation (sample #1–3). These donor corneas were provided by the eye bank of the Hospital Universitario Virgen de la Arrixaca, Murcia, Spain. This study was approved by the Ethical Review Board of both the Hospital and the Universidad de Murcia. Pathological human corneas were obtained from patients undergoing penetrating keratoplasty. They were affected by keratoconus (sample #7–10) and pseudophakic bullous keratopathy (#11). The human samples were treated following the tenets of the Declaration of Helsinki.

Porcine (#4) and bovine (#5) control specimens were obtained from local abattoirs. The use of animal samples was also approved by the Universidad de Murcia Ethical Committee.

Moreover, a model of corneal edema was developed by means of a hyperhydration procedure as described in the following steps. After the set of SHG images was recorded for each control cornea, the glass-bottom dish containing the corneal tissue was filled up with a PBS solution. Samples #4 (porcine), #5 (bovine), and #1 (human) were immersed for 24 hours in that solution to allow swelling and become edematous (samples with edema were respectively renamed as samples #12, #13, and #14). During that interval the samples were not moved from the microscope stage.

An additional set of two corneas from a New Zealand rabbit were provided by the Department of Cellular Biology and Histology of the Universidad de Valladolid, Valladolid, Spain. The left cornea of the animal was chemically burned for 30 seconds with an 8-mm filter paper soaked in NaOH solution (#15). The right eye (#6) was used as control. The animal was sacrificed and the cornea removed after 1 month. The corneal opacity was still readily visible at that time.

All corneas but those with edema (see below) appeared clear during the entire experiment when viewed through a bright-field microscope. For SHG imaging the corneas were placed upside down on a glass-bottom dish. Details on the manipulation and tissue preparation were extensively described in a previous publication.[6]

Healthy samples were imaged at 50 μm within the stroma measured from the Bowman's layer (this was considered as the 0-μm depth location and it was identified as the first axial plane where SHG signal can be detected).[6] Additionally, sample #5 (renamed as #13) was imaged at 0 (control), 5, 7, 20, and 24 hours of hydration in order to perform a temporal

analysis of the edema. Because the entire ocular globe was used for this edema model, the time to induce a significant edema was much longer that when using corneal buttons.[18]

Structure Tensor: Analysis of the Collagen Distribution

To analyze the spatial organization of the collagen fibers of the different corneas, the ST method was applied.[33] This is a mathematic procedure, which provides quantitative information on the orientation of the fibers and the isotropy of the analyzed structure. It is based on the calculation of the partial derivatives along the Cartesian directions, what provides the preferential directions of the image gradient. The resultant matrix is called ST matrix, and the contrast of its eigenvalues (λ_{max} and λ_{min}) is defined as the degree of isotropy (DoI) of the collagen distribution. The preferential orientation (PO) of the collagen fibers is calculated by an algebraic operation that includes those eigenvalues. The distribution of POs is usually presented as a histogram. The structural dispersion (SD) of the collagen fibers is defined as the standard deviation of the PO across the image. Because a linear correlation between DoI and SD parameters has been reported, only the parameter SD was considered here.[33] For a sample composed of fibers quasi-aligned along a PO, SD is less than or equal to 20°. If SD is greater than 40° a nonorganized structure is present. Values in between are representative of a partially organized distribution. The intervals assigned to the different organization groups were not arbitrarily chosen. They were based on both the values of the eigenvalues and the fit of the PO histogram to a Gaussian function (i.e., statistical parameter R^2). Image processing and ST calculations were performed with a custom-built MATLAB (MathWorks, Natick, MA) script.

Results

Figure 1 shows SHG images of two ex vivo healthy human corneas (samples #1 and #2). A fairly regular distribution of the fibers can be observed, what agrees well with previous literature.[4–6]

To quantify the organization of the corneal stroma, the ST was used as indicated in the previous section. The results for the two specimens of Figure 1 are shown in Figure 2. The panels depict the corresponding histograms of PO. These show a distribution around a maximum (i.e., the PO of the collagen fibers), what reveals the presence of an organized structure. This fact is corroborated by the SD values. These are lower than 20°, what indicates that healthy corneas present a low structural dispersion. Results for sample #3 (not shown) are similar (SD = 18°).

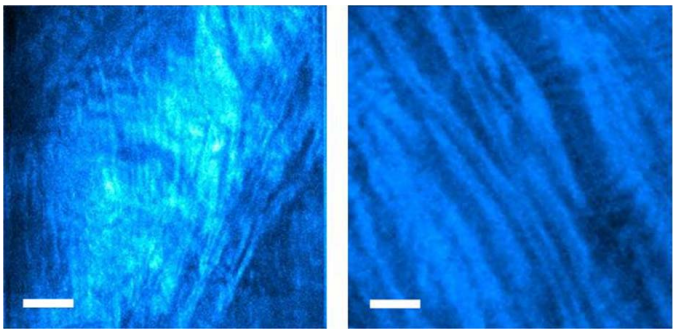

Figure 1. SHG images from two healthy corneas (depth location: 50 μm). *Scale bar*: 50 μm.

The results for the three animal models agree with these findings in control human corneas. In particular, the SD values were 15°, 5°, and 12° for porcine (#4), bovine (#5), and rabbit (#6) samples, respectively. These values are also associated to organized collagen arrangements.

Figure 3 presents SHG images of human corneas affected by pathologies, such as keratoconus (samples #9 and #10) and bullous keratopathy (#11). As expected, the stroma structure of these corneas drastically differs from that of healthy ones shown in Figure 1. A simple visualization indicates an apparent absence of a PO in the collagen fibers. Moreover, for sample #11, the typical cysts observed in a bullous keratopathy are also visualized (see red arrow). The quality of the SHG image allows calculating their dimensions, approximately 38 μm in diameter for this particular sample.

The collagen organization of these corneas has also been quantified through the ST. PO distribution histograms are depicted in Figure 4. These results noticeable differ from those of control samples in Figure 2. For these pathological samples the PO histograms present a fairly uniform distribution without a PO. SD values were always higher than 60°, what indicates that pathological samples present a nonorganized collagen arrangement.

To confirm that pathological corneas suffer changes in collagen distribution that lead to an increase in SD, some corneas were subjected to an edematization process as reported in the Materials and Methods section. This allows the comparison of

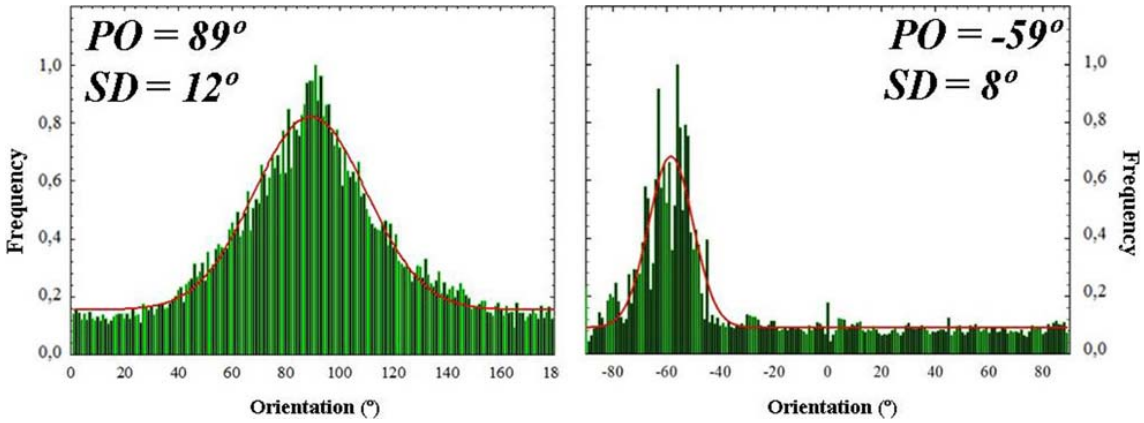

Figure 2. Histograms of PO distribution corresponding to the samples showed in Figure 1. Values of PO and SD are also included.

the lamellar arrangement in the same sample under the following two experimental conditions: healthy (first) and edematous (after swelling by hyperhydration). SHG images were acquired in both conditions and the ST was used to quantify collagen modifications due to the presence of edema. Results for the bovine corneas (samples #5 and #13) are presented in Figure 5.

Whereas the SHG image of the healthy bovine cornea (#5) provides a low SD (5°), the value obtained when this cornea becomes edematous (#13) was noticeably larger (48°). This means that the edema turns the organized structure into a nonorganized one (or randomly distributed). For this sample the healthy control collagen arrangement reveals a PO histogram with a peak approximately at −5°; however, for the edematous cornea, there is a noticeable decrease in SHG signal and a PO does not exist. All this indicates that the inflammatory process occurring during edematization leads to a loss of regular distribution of the lamellae. The SD values obtained for porcine and human edematous corneas (samples #12 and #14) provided also values corresponding to a nonorganized collagen distribution (70° and 60°, respectively).

For the sense of completeness, Figure 6 shows a plot containing the temporal evolution of the ST for the edematous cornea of the previous figure. The induced edema (see Materials and Methods above) shows the progressive collagen disorganization (in a plane located 50 μm behind the Bowman's layer) as a result of the swelling produced during 24 hours. This model makes evident that the ST method is also able to detect intermediate states during the edema progression.

Figure 7 compares a rabbit cornea before and after being damaged with NaOH solution (see Materials and Methods). Once again, the difference between both collagen distributions is readily visible (apart

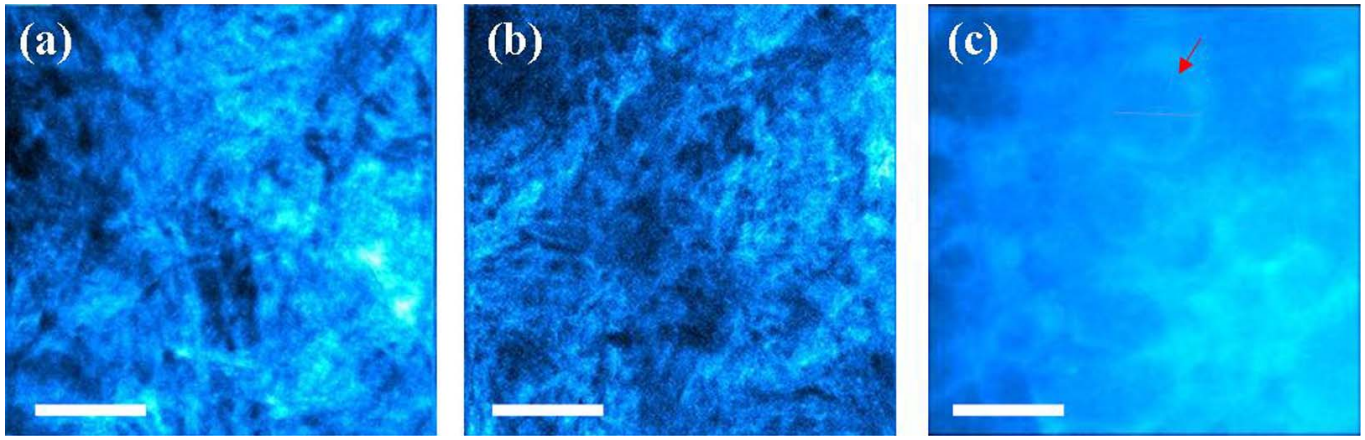

Figure 3. SHG images of ex vivo pathological corneas (depth location: 50 μm): keratoconus (a, b) and bullous keratopathy (c). *Scale bar*: 50 μm.

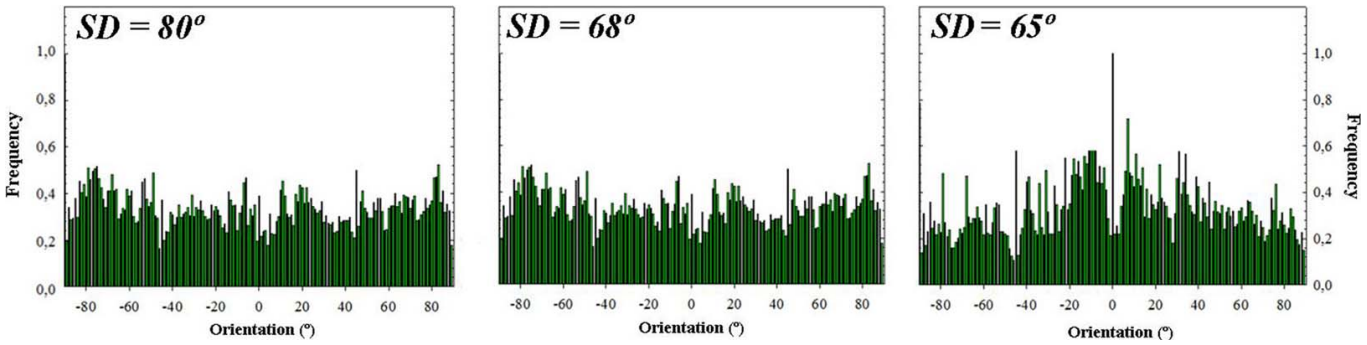

Figure 4. Histograms of PO distribution corresponding to the samples shown in Figure 3.

from the significant reduction in SHG signal). The PO histograms turn from presenting a clear PO (~90°) to a uniform distribution without a PO. Accordingly, the SD increases from 12° to 62°.

As a general visualization of these results, for all samples here used, Figure 8 depicts the SD values computed with the ST. From this plot it can be observed that all pathological samples presented SD values above 40° (anterior stroma location). On the contrary, healthy corneas showed SDs below 20°. This plot serves as a "proof of concept" to numerically differentiate healthy from pathological corneas.

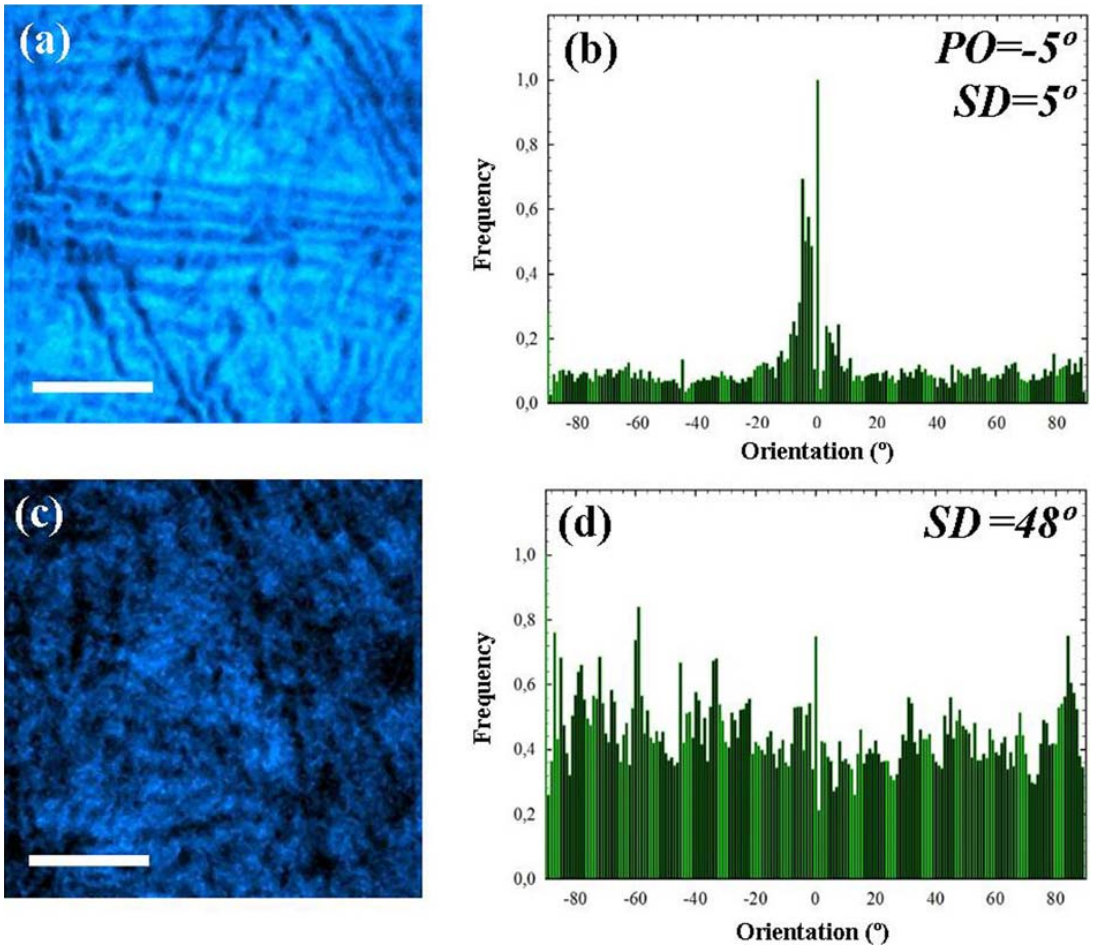

Figure 5. SHG images of a control (a) and edematous bovine cornea (c); PO distribution histograms (b, d). *Bar length*, 50 μm. SHG images share the same color scale for a direct comparison. The depth location was 50 μm.

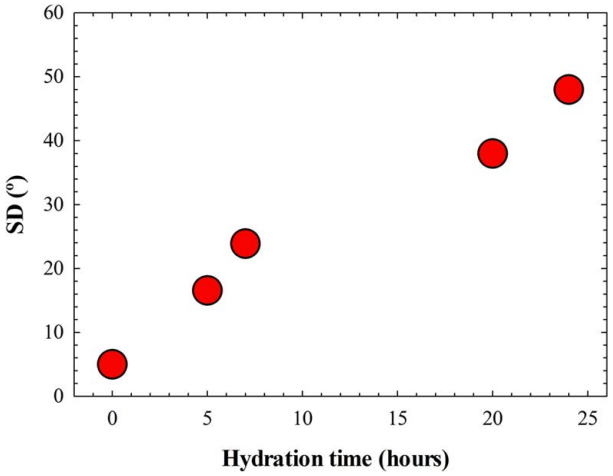

Figure 6. Changes in SD as a function of time for an edematous bovine cornea. Maximum and minimum values correspond to the plots in Figure 5.

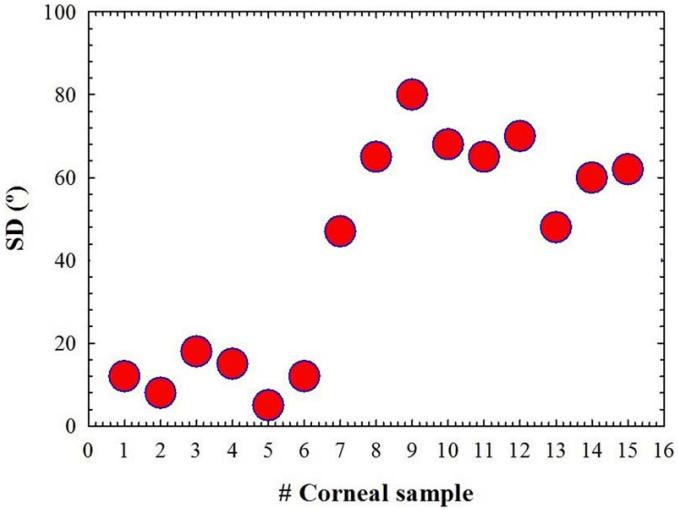

Figure 8. SD values for all the corneal tissues involved in the experiment.

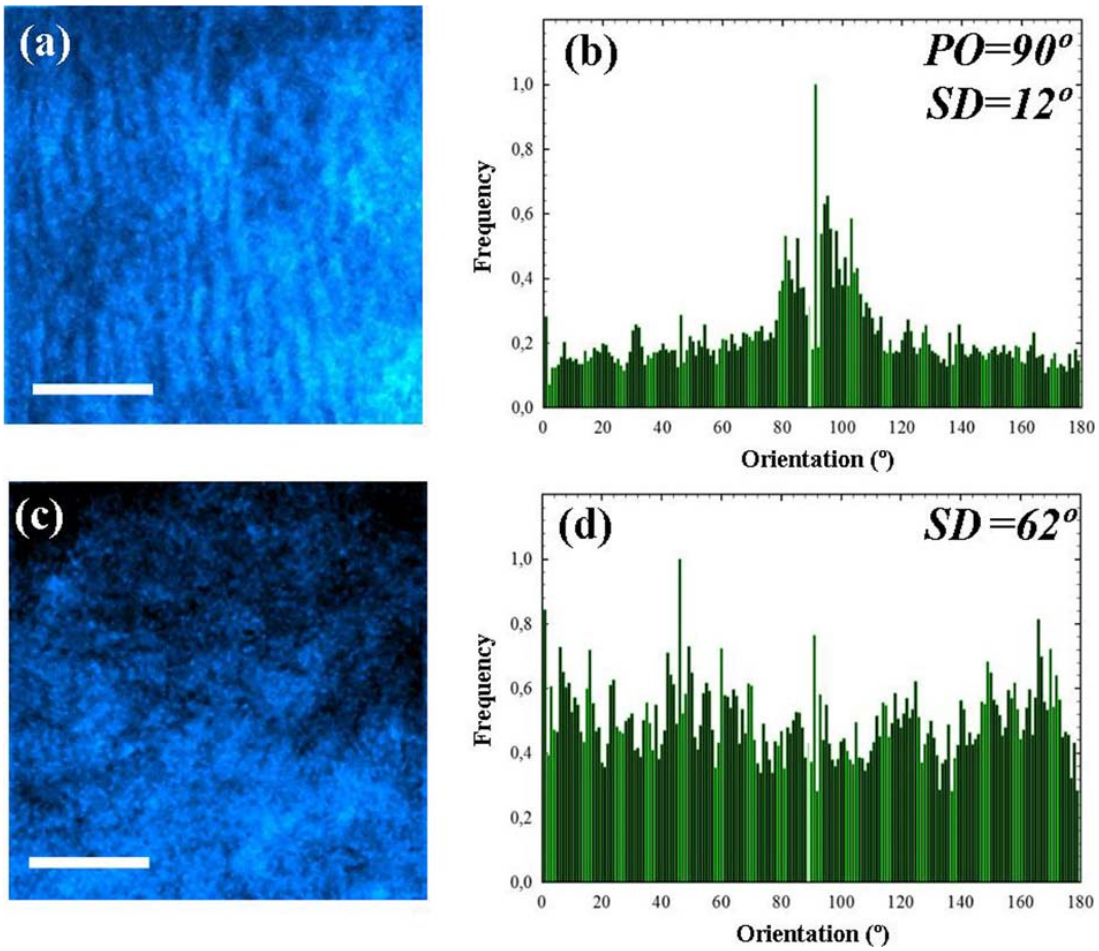

Figure 7. SHG images of a control (a) and "burned" rabbit cornea (c); PO distribution histograms (b, d). Depth location, 50 μm. SHG images share the same color scale for a direct comparison. The *scale bar* corresponds to 50 μm.

Discussion

Because corneal diseases can lead to severe vision loss, characterization and noninvasive analyses of the stromal collagen arrangement are of great importance. During the last decade there has been an increasing interest in using SHG microscopy to discriminate healthy from pathological corneas. In the present work, the so-called ST has been applied to SHG images to quantitatively differentiate healthy from pathological corneas. The approach provides numeric parameters (SD and PO) that can be used as an objective and useful tool in corneal disease discrimination.

Results herein show that control (healthy) tissues reveal a regular distribution of collagen fibers within the anterior stroma. In terms of the SD, the values were always smaller than 20°, what indicates the presence of a fairly well-organized structure. In the PO histograms a dominant direction of the fibers can also be observed (see for instance Fig. 2). On the contrary, SD values were larger than 40° in all the pathological samples. Accordingly, the histograms of PO showed homogeneous distributions with absence of a significant preferential orientation.

Qualitative changes between normal and keratoconic human corneas were early described using SHG microscopy.[10,35] Structural alterations were later quantified by means of the FFT.[11] The parameter known as the aspect ratio (AR; defined as the quotient between the short and the long axes of the ellipse fitting the FT spectrum of the image) was used. AR was shown to provide statistically different values between control and pathological samples. Using SHG images of the anterior stroma (up to 30 μm below the Bowman's membrane), Mercatelli et al.[13] reported a three-dimensional correlation analysis after FFT calculation to discriminate healthy from keratoconic corneas. In a more recent experiment, Batista et al.[14] used the peak prominence of the main orientation computed through the FFT. They reported a decrease in this parameter when control and keratoconic corneas were compared (deepest location ~65 μm). The present results agree with these literatures. Moreover, structural differences at the anterior stroma have also been found when using the proposed ST method.

The changes in the collagen arrangement of the anterior stroma of an edematous sample have also been studied. Normal and edematous corneas (after 24 hours of hyperhydration) present different collagen distribution (see Fig. 5) as assessed with the ST. This fact was also previously reported at the anterior stoma by measuring the fibrillar interspacing and the lamellar thickness.[18] In addition, an evaluation of the temporal evolution of the stromal organization has also been carried out for completeness. The study shows that the SD parameter increases as a function of the hydration time (see Fig. 6), which is coherent with the results of Hsueh et al.[18]

Although SHG imaging has also been used to analyze other corneal pathologies, such as bullous keratopathy[19,20] or keratitis,[15–17] a numeric parameter to objectively indicate the existence of pathology has not been clearly provided. Our results are coherent with those previous qualitative data in the sense that diseased samples present marked abnormalities in the arrangement of the collagen lamellae. A few representative examples of corneal pathologies have been presented along this work (keratoconus, edema, and bullous keratopathy). However, the procedure can also be applied to corneal tissues suffering from other diseases, such as infectious keratitis,[14–17] fibrosis,[21,22] scars,[14,36] and diabetes mellitus.[37]

Moreover, a chemically damaged cornea was also involved in the study. These specimens were compared with control corneas. Our findings show that whereas the SD at the anterior stroma of damaged specimens was above 40°, the value for the control corneas was below 20°. This corroborates that pathological samples can be quantified through the SD as collagen-based structures with a low degree of organization. In this sense, quantization and objective analyses of corneas after surgery,[26,31,32,38–40] with intraocular pressure disorders[41,42] and physical trauma[24,43] might also benefit from this tool.

Many of the previous experiments that evaluated the collagen arrangement in a quantitative manner employed the FFT and some parameters derived from it. Although very useful and widely applied, this algorithm usually combines analytical and manual schemes. Image filtering (usually before and after FFT calculation) to adjust contrast and to smooth the image must often be used. This makes this procedure be operator-dependent and some results might be biased or misleading. In addition, the FTT method might also fail when complex collagen patterns (highly wavy, interweaving, crosshatching, etc.) are involved.[25] In particular, the use of the AR might erroneously identify a crosshatched structure as a random distribution. Some of these limitations are over-passed when using the ST algorithm.

Although it is known that corneal changes occurring under certain pathologies or external damage might be depth-dependent, the main goal of

this work was not a three-dimensional analysis of pathological corneas. Instead, we just used SHG images from the anterior stroma where changes in the collagen distribution due to different pathologies are known to be present.[13,14,18,25,43] The ST was applied to those (single plane) images to distinguish healthy from diseased collagen patterns.

SHG imaging offers inherent confocality and provides depth-resolved information in both healthy and pathological corneas. In particular, the ST has recently been shown to be very sensitive to changes in fiber orientation with depth in postsurgery (cross-linked) corneas.[44]

In summary, the proposed method is a reliable and useful tool to detect and quantify structural changes produced in pathological corneas. This is a proof of concept that provides an experimental "objective score" to discriminate control from pathological or damaged corneas. A significant increase in the amount of analyzed samples might help to establish a "pathological threshold" in the future. This method applied to ex vivo specimens represents a first step. The implementation of this technique in a clinical research instrument for the measurement of living human eyes[45] might represent a promising tool in ophthalmology, especially in monitoring corneal pathologies, or in the following-up of surgically altered corneas.

Acknowledgments

Supported by the Secretaría de Estado de Investigación, Desarrollo e Innovación, Spain (Grant No. FIS2016-76163-R), the European Research Council Advanced Grant ERC-2013-AdG-339228 (SEECAT), and the "Fundación Séneca," Murcia, Spain.

Presented in part at the Annual Meeting of the Association for Research in Vision and Ophthalmology, Seattle, Washington, May 2016.

Disclosure: **F.J. Ávila**, None; **P. Artal**, None; **J.M. Bueno**, None

References

1. Maurice DM. The structure and transparency of the cornea. *J Physiol*. 1957;136:263–286.
2. Quantock AJ, Winkler M, Parfitt GJ, et al. From nano to macro: studying the hierarchical structure of the corneal extracellular matrix. *Exp Eye Res*. 2015;133:81–99.
3. Meek KM, Hayes S. Corneal cross-linking - a review. *Ophthalmic Physiol Opt*. 2013;33:78–93.
4. Morishige N, Petroll WM, Nishida T, Kenney MC, Jester JV. Noninvasive corneal stromal collagen imaging using two-photon-generated second-harmonic signals. *J. Cataract Refract Surg*. 2006;32:1784–1791.
5. Aptel F, Olivier N, Deniset-Besseau A, et al. Multimodal nonlinear imaging of the human cornea. *Invest Ophthalmol Vis Sci*. 2010;51:2459–2465.
6. Bueno JM, Gualda EJ, Artal P. Analysis of corneal stroma organization with wavefront optimized nonlinear microscopy. *Cornea*. 2011;30:692–701.
7. Morishige N, Takagi Y, Chikama T, Takahara A, Nishida T. Three-dimensional analysis of collagen lamellae in the anterior stroma of the human cornea visualized by second harmonic generation imaging microscopy. *Invest Ophthalmol Vis Sci*. 2011;52:911–915.
8. Winkler M, Chai D, Kriling S, et al. Nonlinear optical macroscopic assessment of 3-D corneal collagen organization and axial biomechanics. *Invest Ophthalmol Vis Sci*. 2011;52:8818–8827.
9. Gibson EA, Masihzadeh O, Lei TC, Ammar DA, Kahook MY. Multiphoton microscopy for ophthalmic imaging. *J Ophthalmol*. 2011;2011:870879.
10. Tan HY, Sun Y, Lin SJ, et al. Multiphoton fluorescence and second harmonic generation imaging of the structural alterations in keratoconus ex vivo. *Invest Ophthalmol Vis Sci*. 2006;47:5251–5259.
11. Lo W, Chen WL, Hsueh CM, et al. Fast Fourier transform-based analysis of second-harmonic generation image in keratoconic cornea. *Invest Ophthalmol Vis Sci*. 2012;53:3501–3507.
12. Morishige N, Shin-gyou-uchi R, Azumi H, et al. Quantitative analysis of collagen lamellae in the normal and keratoconic human cornea by second harmonic generation imaging microscopy. *Invest Ophthalmol Vis Sci*. 2014;55:8377–8385.
13. Mercatelli R, Ratto F, Rossi F, et al. Three-dimensional mapping of the orientation of collagen corneal lamellae in healthy and keratoconic human corneas using SHG microscopy. *J Biophtonics*. 2017;10:75–83.
14. Batista A, Breunig HG, König A, et al. High-resolution, label-free two-photon imaging of

diseased human corneas. *J Biomed Opt*. 2018;23: 036002.
15. Tan HY, Sun Y, Lo W, et al. Multiphoton fluorescence and second harmonic generation microscopy for imaging infectious keratitis. *J Biomed Opt*. 2007;12:024013.
16. Lee JH, Lee S, Yoon CJ, et al. Comparison of reflectance confocal microscopy and two-photon second harmonic generation microscopy in fungal keratitis rabbit model ex vivo. *Biomed Opt Express*. 2016;7:677–687.
17. Robertson DM, Rogers NA, Petroll WM, Zhu M. Second harmonic generation imaging of corneal stroma after infection by Pseudomonas aeruginosa. *Sci Rep*. 2017;7:46116.
18. Hsueh CM, Lo W, Chen WL, et al. Structural characterization of edematous corneas by forward and backward second harmonic generation imaging. *Biophysical J*. 2009;97:1198–1205.
19. Morishige N, Yamada N, Zhang X, et al. Abnormalities of stromal structure in the bullous keratopathy cornea identified by second harmonic generation imaging microscopy. *Invest Ophthalmol Vis Sci*. 2012;53:4998–5003.
20. Grieve K, Kate D, Ghoubay C, et al. Stromal striae: a new insight into corneal physiology and mechanics. *Sci Rep*. 2017;7:13584.
21. Morishige N, Yamada N, Teranishi S, Chikama T, Nishida T, Takahara A. Detection of subepithelial fibrosis associated with corneal stromal edema by second harmonic generation imaging microscopy. *Invest Ophthalmol Vis Sci*. 2009;50: 3145–3150.
22. Farid M, Morishige N, Lam L, Wahlert A, Steinert RF, Jester JV. Detection of corneal fibrosis by imaging second harmonic-generated signals in rabbit corneas treated with mitomycin C after excimer laser surface ablation. *Invest Ophthalmol Vis Sci*. 2008;49:4377–4383.
23. Cicchi R, Vogler N, Kapsokalyvas D, et al. From molecular structure to tissue architecture: collagen organization probed by SHG microscopy. *J Biophotonics*. 2013;6:129–142.
24. Matteini P, Ratto F, Rossi F, et al. Photothermally-induced disordered patterns of corneal collagen revealed by SHG imaging. *Opt Express*. 2009;17:4868–4878.
25. Bueno JM, Palacios R, Chessey MK, Ginis H. Analysis of spatial lamellar distribution from adaptive-optics second harmonic generation corneal images. *Biomed Opt Express*. 2013;4:1006–1013.
26. Germann JA, Martinez-Enriquez E, Marcos S. Quantization of collagen organization in the stroma with a new order coefficient. *Biomed Opt Express*. 2018;9:173–189.
27. Batista A, Breunig HG, König A, et al. Assessment of human corneas prior to transplantation using high-resolution two-photon imaging. *Invest Ophthalmol Vis Sci*. 2018;59:176–184.
28. Lombardo M, Merino D, Loza-Alvarez P, Lombardo G. Translational label-free nonlinear imaging biomarkers to classify the human corneal microstructure. *Biomed Opt Express*. 2015;6: 2803–2818.
29. Lombardo M, Serrao S, Barbaro V, et al. Multimodal imaging quality control of epithelia regenerated with cultured human donor corneal limbal epithelial stem cells. *Sci Rep*. 2017;7: 515401–515410.
30. Mega Y, Robitaille M, Zareian R, et al. Quantification of lamellar orientation in corneal collagen using second harmonic generation images. *Opt Lett*. 2012;37:3312–3314.
31. Tan HY, Chang YL, Lo W, et al. Characterizing the morphologic changes in collagen crosslinked–treated corneas by Fourier transform–second harmonic generation imaging. *J Cataract Refract Surg*. 2013;39:779–788.
32. Gupta P, Anyama B, Edward K, et al. Depth resolved differences after corneal crosslinking with and without epithelial debridement using multimodal imaging. *Trans Vis Sci Tech*. 2014; 3(4):51–58.
33. Ávila FJ, Bueno JM. Analysis and quantification of collagen organization with the structure tensor in second harmonic microscopy images of ocular tissues. *Appl Opt*. 2015;54:9848–9854.
34. Bueno JM, Giakoumaki A. Gualda EJ, et al. Analysis of the chicken retina with an adaptive optics multiphoton microscope. *Biomed Opt Express*. 2011;2:1637–1648.
35. Morishige N, Wahlert AJ, Kenney MC, et al. Second-harmonic imaging microscopy of normal human and keratoconus cornea. *Invest Ophthalmol Vis Sci*. 2007;48:1087–1094.
36. Teng SW, Tan HY, Sun Y, et al. Multiphoton fluorescence and second-harmonic-generation microscopy for imaging structural alterations in corneal scar tissue in penetrating full-thickness wound. *Arch Ophthalmol*. 2007;125:977–978.
37. Tseng JY, Ghazaryan AA, Lo W, et al. Multiphoton spectral microscopy for imaging and quantification of tissue glycation. *Biomed Opt Express*. 2011;2:218–230.
38. Wang TJ, Lo W, Hsueh CM, et al. Ex vivo multiphoton analysis of rabbit corneal wound

healing following conductive keratoplasty. *J Biomed Opt*. 2008;13:034019.
39. Bueno JM, Gualda EJ, Giakoumaki A, et al. Multiphoton microscopy of ex vivo corneas after collagen cross-linking. *Invest Ophthalmol Vis Sci*. 2011;52:5325–5331.
40. Bueno JM, Palacios R, Pennos A, Artal P. Second-harmonic generation microscopy of photocurable polymer intrastromal implants in ex-vivo corneas. *Biomed Opt Express*. 2015;6:2211–2219.
41. Wu Q, Yeh AT. Rabbit cornea microstructure response to changes in intraocular pressure visualized by using nonlinear optical microscopy. *Cornea*. 2008;27:202–208.
42. Wu Q, Applegate BE, Yeh AT. Cornea microstructure and mechanical responses measured with nonlinear optical and optical coherence microscopy using sub-10-fs pulses. *Biomed Opt Express*. 2011;2:1135–1146.
43. Lo W, Chang YL, Liu JS, et al. Multimodal, multiphoton microscopy and image correlation analysis for characterizing corneal thermal damage. *J Biomed Opt*. 2009;14:054003.
44. Bueno JM, Ávila FJ, Martínez-García MC. Quantitative analysis of the corneal collagen distributiuon after in vivo cross-linking with second harmonic microscopy. *Biomed Res Int*. 2019;2019:3860498.
45. Artal P, Ávila FJ, Bueno JM. Second harmonic generation microscopy of the living human cornea. *Proc SPIE*. 10498, Multiphoton Microscopy in the Biomedical Sciences XVIII, 1049810 (23 February 2018).